Mon. Not. R. Astron. Soc. **293,** 60–70 (1998)

Measuring the power spectrum of density fluctuations at intermediate redshift with X-ray background observations

X. Barcons,[1,2] A. C. Fabian[1] and F. J. Carrera[2]

[1]*Institute of Astronomy, Madingley Road, Cambridge CB3 0HA*
[2]*Instituto de Física de Cantabria (Consejo Superior de Investigaciones Científicas – Universidad de Cantabria), 39005 Santander, Spain*

Accepted 1997 September 5. Received 1997 August 15; in original form 1997 May 28

ABSTRACT

The precision of intensity measurements of the extragalactic X-ray background (XRB) on an angular scale of about a degree is dominated by spatial fluctuations caused by source confusion noise. X-ray source counts at the flux level responsible for these fluctuations, $\sim 10^{-12}$ erg cm^{-2} s^{-1}, will soon be accurately measured by new missions, and it will then be possible to detect the weaker fluctuations caused by the clustering of the fainter, more distant sources which produce the bulk of the XRB. We show here that measurements of these excess fluctuations at the level of $(\Delta I/I) \sim 2 \times 10^{-3}$ are within reach, improving by an order of magnitude on present upper limits. Since it is likely that most (if not all) of the XRB will be resolved into sources by *AXAF*, subsequent optical identification of these sources will reveal the X-ray volume emissivity in the Universe as a function of redshift. With these ingredients, all-sky observations of the XRB can be used to measure the power spectrum (PS) of the density fluctuations in the Universe at comoving wavevectors $k_c \sim 0.01$–0.1 Mpc^{-1} at redshifts where most of the XRB is likely to originate ($z \sim$ 1–2) with a sensitivity similar to, or better than, the predictions from large-scale structure theories. A relatively simple X-ray experiment, carried out by a large-area proportional counter with a 0.5–2 deg^2 collimated field of view scanning the whole sky a few times, would be able to determine the PS of the density fluctuations near its expected peak in wavevector with an accuracy better than 10 per cent.

Key words: methods: statistical – diffuse radiation – large-scale structure of Universe – X-rays: general.

1 INTRODUCTION

1.1 The X-ray background and the large-scale structure of the Universe

35 years of study after its discovery by Giacconi et al. (1962), the X-ray background (XRB) has proven to be a valuable tool in the study of the large-scale structure (LSS) of the Universe. A significant fraction of the XRB (particularly at soft energies) is now resolved into sources, the vast majority of which are extragalactic. The deepest surveys carried out with *ROSAT* (see, e.g., Hasinger 1996 for a recent review) resolved about 60 per cent of the 0.5–2 keV XRB into mostly active galactic nuclei (AGN) and other X-ray-luminous galaxies (particularly narrow-line X-ray-emitting galaxies – NLXGs). The X-ray volume emissivity of these objects rises rapidly from redshift $z=0$ to $z=1$–2, above which it appears to decline. It is at redshifts of 1–2 where the bulk of the resolved soft XRB originates. Preliminary work on *ASCA* observations (Georgantopoulos et al. 1997) hints that something similar is happening at harder energies, although the fraction of the XRB resolved is lower and the sources are much more difficult to identify due to the limited spatial resolution of *ASCA*.

Isotropy arguments at soft X-ray energies (see, e.g., Carrera, Fabian & Barcons 1997) show that a good deal of the unresolved fraction of the soft XRB has to come from redshifts $z>1$. It is then concluded that the bulk of the XRB originates precisely at the epoch where the largest present-day structures collapse and where different cosmological models give the most different predictions.

Any cosmological model has to confront two basic boundary conditions: (1) the Universe was very smooth at $z=1500$ where the cosmic microwave background (CMB) was produced, and (2) the Universe is very lumpy and rich in structure today ($z=0$). Density fluctuations in the Universe grow linearly from the highly homogeneous CMB recombination epoch until they become non-linear at low redshifts and collapse to form the LSS we see today. The redshift at which a density fluctuation becomes non-linear depends on the spatial scale of the fluctuation and on the cosmological model, but for the most popular models this happens at a typical redshift $z\sim1$–5 for scales of 10–100 h^{-1} Mpc ($H_0=100\ h$ km s^{-1} Mpc^{-1}, $q_0=0.5$ and $\Lambda=0$ are used throughout unless otherwise explicitly stated). Studies of the XRB as proposed here will add a further constraint to cosmological models, since they will measure the power spectrum (PS) of the fluctuations at comoving wavevectors $k_c\sim0.01$–$0.1\ h$ Mpc^{-1} with sufficient sensitivity to constrain cosmological scenarios. In particular, the parameters governing the evolution of the PS (e.g., q_0) could be constrained by these observations.

Mapping the structure of the Universe at intermediate redshifts with X-rays has the added bonus that the objects presumably occur in the highest density regions. Indeed, cosmic X-ray sources require strong gravity to be switched-on (either very extended potential wells, as in galaxy clusters, or very deep ones as in AGN), and therefore the X-ray sources existing at intermediate redshifts could actually correspond to the objects that first formed in the Universe at even earlier epochs. A possible indication of this is in the 'bias factor' for X-ray sources; there is some evidence that this has a high value, at least for the nearby luminous X-ray sources (see, e.g., Miyaji 1995 and Boughn, Crittenden & Turok 1997, who find values larger than 5). Although direct studies of the clustering of X-ray-selected AGN (Boyle & Mo 1993; Carrera et al. 1997) show that these values might be too large for lower luminosity objects, bias factors of 2 or 3 might be likely for X-ray sources. This issue will be resolved with *ABRIXAS* when the dipole of the distribution of sources is compared to the XRB dipole.

Parallel studies at other wavelengths are currently being used to extract information about LSS at high redshift. Deep galaxy surveys, especially the Canada–France Redshift Survey, are showing how the galaxy–galaxy correlation function evolves up to redshifts close to 1 (Le Fèvre et al. 1996). However, scales of the order $\sim100\ h^{-1}$ Mpc are beyond the scope of such work. High-redshift clustering is also being investigated by means of different classes of QSO absorption systems (Fernández-Soto et al. 1996; Cristiani et al. 1997). None of these studies provides clear evidence on how clustering in the Universe evolves. Again, scales in excess of 10 h^{-1} Mpc are not easily accessible by these studies. QSO clustering appears to be a realistic way to map large-scale structure at high redshift, although the scales we are dealing with here are also difficult to study with existing samples (see, e.g., Croom & Shanks 1996). However, analyses of the spatial structure of deep radio surveys (at a redshift $z\sim1$) do appear promising (Cress et al. 1996; Loan, Wall & Lahav 1997).

Unless otherwise stated, the above cosmological parameters will be used throughout and X-ray fluxes will be referred to the 2–10 keV bandpass.

1.2 Deep versus wide-area surveys

The next generation of X-ray instruments to be operating in the next decade are mostly based on X-ray imaging, with grazing-incidence X-ray telescopes working up to energies ~10 keV. This is indeed necessary to unveil the origin of the XRB, since it should not be forgotten that most of the XRB energy density resides at 30 keV, whereas most of our knowledge on the source content is so far limited to energies below 3 keV, where only a few per cent of the total energy budget is contained. It is then essential to carry out imaging surveys at as high an energy as possible, and to identify the sources dominating the source counts.

X-ray-imaging telescopes are well suited to medium and deep surveys. Their limited effective collecting area calls for long integration times to reduce photon counting noise, resulting in very deep images, eventually down to the confusion limit. We discuss some of these missions and their relation to the present work in the next subsection. The source counts (the so-called $\log N$–$\log S$ relation) are then determined down to very faint fluxes in a small solid angle and therefore with limited precision. If exposures are long enough, so that confusion noise dominates over photon counting noise, a fluctuation analysis provides an extension of the $\log N$–$\log S$ curve for almost another decade in flux downwards.

An alternative way of using an X-ray telescope with a suitable imaging detector is by doing a shallow all-sky survey. This was done by *ROSAT* at soft X-ray energies (Voges 1993) and will be done by *ABRIXAS* up to 10 keV (Friedrich et al. 1996). Typical exposure times are then short, and photon counting noise is the limiting factor. Such an experiment is able to produce a map with accurate positions of the brightest sources over the whole sky. One can then extract much information about the cosmographical distribution of the sources and the local LSS of the Universe.

The method we propose here requires the whole sky to be surveyed (to achieve the best statistics) to measure the PS of the density fluctuations with negligible photon counting noise. In order to avoid the strongest structures associated with the Galaxy, only photon energies above 2 keV will be considered (see discussion in Section 4). A diffuse Galactic component, amounting to <10 per cent, associated with the Galaxy has been detected (Warwick, Pye & Fabian 1980; Iwan et al. 1982), but it is expected to be smooth on scales of a degree and therefore will not contribute to the fluctuations. We therefore focus on non-imaging instruments in order to obtain a large effective collecting area, such that, in a typical exposure of about 100 s, confusion noise (i.e., the fluctuations in the sky brightness caused by the presence of the sources) exceeds photon counting noise. The field of view cannot be collimated to much less than 1 deg^2 to maintain the required low photon counting noise level. The most clear example of such an experiment was the *HEAO-1 A2* experiment, and, as an instrument, the *Ginga* Large-Area Proportional Counter (LAC), which, unfortunately for the purposes of this paper, did not carry out an all-sky survey.

For a homogeneous distribution of sources, the sky brightness fluctuations on scales of a few degrees will be dominated by relatively bright ($\sim10^{-12}$ erg cm^{-2} s^{-1}) nearby sources (see Section 2 for details). However, cluster-

ing of sources, if strong enough, can be visible out to higher redshifts. The reason is that if several or many distant faint X-ray sources cluster within the scale of a field of view, they will produce a large enough signal in the distribution of X-ray sky intensities. As it will be shown later, the imprint of inhomogeneities in the distribution of X-ray sources on the excess fluctuations is weighted by the redshift dependence of their X-ray volume emissivity. This means that fluctuations in excess of confusion noise produced by the bright, just unresolved, sources will be most detectable at the redshifts where the bulk of the XRB originates.

It should also be emphasized, and this has been proven by similar analyses on existing data, that, besides having a negligible photon counting noise, what determines the sensitivity in the measurement of excess fluctuations is the number of independent observations – as will be shown later, $(\Delta I/I)_{2\sigma} \propto N_{\rm obs}^{-1/2}$, $N_{\rm obs}$ being the number of sky positions where the XRB intensity has been measured. All-sky coverage is then essential.

1.3 X-ray missions relevant to the present work

There are a number of previous, existing and planned missions which have made, or are expected to make, decisive steps towards the goal that is pursued here. Among them, the *HEAO-2 A2* all-sky experiment has proven to be the most useful for cosmological work (Boldt 1987), since it provided all-sky coverage with small photon counting noise. X-ray *HEAO-1 A2* maps have been used to measure the XRB dipole (Shafer 1983; Shafer & Fabian 1983; Lahav, Piran & Treyer 1997), maybe also higher order multipoles (Lahav, private communication), the search for the Great Attractor (Jahoda & Mushotzky 1989), cosmography of voids (Mushotzky & Jahoda 1992) and superclusters (Persic et al. 1990), and many other cosmologically relevant issues. Many things have been learned from that experiment, and in particular that an absolute determination of sky brightness requires a combination of two different fields of view. It will be shown here that when other data become available, the *HEAO-1 A2* observations will enable a decisive step forward to be made in the measurement of the PS at intermediate redshift.

As mentioned before, the *Ginga* LAC, with a field of view of $\sim 1° \times 2°$ and a larger effective area, could have provided a very accurate measurement of the PS at high redshift if it had carried out an all-sky survey. Also, it was rather unfortunate for the present purposes that the *Ginga* LAC had all collimators with the same angular size, and therefore the non-cosmic XRB had to be modelled (as opposed to subtracted). Nevertheless, even with the data available, very interesting constraints on LSS were found (Carrera et al. 1991, 1993).

In this paper we propose to measure or constrain the excess fluctuations by improving the precision of the confusion noise produced by relatively nearby bright sources. That means that the source counts down to fluxes $< 10^{-12}$ erg cm^{-2} s^{-1} need to be obtained with high accuracy. This relation is only known today from fluctuation analyses of *HEAO-1 A2* (Shafer 1983) and *Ginga* LAC data (Hayashida 1989; Butcher et al. 1997). More recently, *ASCA* surveys (Inoue et al. 1996; Georgantopoulos et al. 1997) have measured the source counts at fluxes $\sim 10^{-14}$ erg cm^{-2} s^{-1}. However, these results are based on small solid angles, and therefore the normalization of the source counts is uncertain.

A forthcoming mission that will define the $\log N$–$\log S$ relation at 10^{-12} erg cm^{-2} s^{-1} fluxes with the highest accuracy is *ABRIXAS*. This is because *ABRIXAS* will detect all sources in the sky brighter than this flux. A discussion of the accuracy in the modelling of confusion noise enabled by *ABRIXAS* is presented in Section 2.

The next most important mission for the proposed experiment is *XMM*. *XMM* will not only define the $\log N$–$\log S$ at fainter fluxes, but, most importantly, will find the X-ray spectrum of the sources that contribute to both the confusion noise and the excess fluctuations down to very faint fluxes. *XMM* will also be measuring or constraining the power spectrum of the fluctuations at comoving wavevectors $k_{\rm c} \sim 0.1$–$1\ h$ Mpc^{-1}, thus complementing the observations at larger scales.

Finally, *AXAF* may resolve the whole XRB at ~ 1 keV. The superb X-ray angular resolution combined with large optical telescopes will provide a direct insight into the evolution of the X-ray volume emissivity of the sources producing virtually all the XRB, which is one of the key inputs to model excess fluctuations in terms of source clustering.

1.4 Organization of the paper

In Section 2 we parametrize the noise components and sensitivities relevant to the measurement of excess fluctuations by a collimated field-of-view proportional counter. Photon counting noise is estimated in terms of cosmic and non-cosmic backgrounds, based on *Ginga* LAC and *RXTE* observations. Confusion noise is modelled according to our best (rather inaccurate) knowledge of the source counts at 10^{-12} erg cm^{-2} s^{-1}. Particular attention is paid to the issue of the uncertainties and biases that source variability might introduce in that modelling. We show that $(\Delta I/I)_{2\sigma} \sim 2 \times 10^{-3}$ might be reachable with the *HEAO-1 A2* maps when *ABRIXAS* source counts become available.

Section 3 presents the relation between excess fluctuations and the PS. Assuming that the 2–10 keV redshift evolution of the volume emissivity is similar to the one associated with the resolved component of the soft XRB (mostly contributed by QSOs and NLXGs), we demonstrate that sensitive measurements of the PS at $z \sim 1$–2 on comoving wavevectors $k_{\rm c} \sim 0.01$–$0.1\ h$ Mpc^{-1} can be achieved with a few-degree collimator, such as *HEAO-1 A2*. This corresponds to a PS signal below that expected from cold dark matter (CDM) models, which could therefore be accurately tested when reliable information on the 2–10 keV X-ray volume emissivity (presumably from *AXAF* optical identification of deep fields) becomes available.

Section 4 presents a more detailed study of what could be achieved with a new X-ray mission surveying the whole sky with a ~ 0.5–2 deg^2 beam. Using expected future information on the X-ray volume emissivity, such an experiment would be able to measure the PS at intermediate redshift with great accuracy at comoving wavevectors $k_{\rm c} \sim 0.01$–$0.1\ h$ Mpc^{-1}. Specifically, constraints on the evolutionary parameters of the PS (and in particular q_0) at the redshifts involved

could be found. Such a mission would provide other scientific results which are also outlined in that section.

In Section 5 we summarize our results.

2 SENSITIVITY OF XRB OBSERVATIONS TO EXCESS FLUCTUATIONS

For a uniform distribution of X-ray sources, the distribution of spatial fluctuations in the XRB, when observed through a given beam, can be predicted if the source counts and the noise components (particularly photon counting noise) are known. This is well documented (Scheuer 1957, 1974; Condon 1974; Shafer 1983) and has been applied many times with success to derive X-ray source counts from XRB fluctuations (Shafer 1983; Hamilton & Helfand 1987; Barcons & Fabian 1990; Hasinger et al. 1993; Barcons et al. 1994; Butcher et al. 1997). Under the assumption of a uniform distribution of sources in the sky and of confusion noise (i.e., the noise coming from the presence or absence of sources) dominating over photon counting noise, the distribution of XRB fluctuations [the so-called $P(D)$ curve] is sensitive only down to a flux where there is about one source per beam, and its width (standard deviation) is dominated by the sources of which there are a few (this number depends on the slope of the source counts; see below) per beam. When photon noise is important, the total intrinsic dispersion of the intensity distribution is then

$$\left(\frac{\Delta I}{I}\right)_{\rm intrinsic} = \frac{(\sigma_{\rm c}^2+\sigma_{\rm ph}^2)^{1/2}}{I_{\rm XRB}}, \tag{1}$$

where $\sigma_{\rm c}$ is the confusion noise, $\sigma_{\rm ph}$ is the photon counting noise, and $I_{\rm XRB}$ is the XRB intensity. As a practical issue, we should emphasize that an overall fit to the $P(D)$ curve is mostly sensitive to its second moment, but it has the advantage over the variance that it is not dominated by the brightest unresolved sources [i.e., the tail of the $P(D)$], but by the sources where there are a few per beam.

Now, when the sources are *not* uniformly distributed, but are clustered in the sky, the situation is different. The predicted $P(D)$ distribution then needs all of the n-point correlation functions, for n at least as large as the *total* average number of sources per beam (Barcons 1992). There are indeed models for the n-point correlation function of objects (e.g., a simple Gaussian model where all correlation functions beyond $n=2$ are zero, or a model where there is a random distribution of clusters of sources, all of them with the same average profile which determines the n-point correlation functions), but observationally there is little knowledge of them beyond $n=3$.

The contribution of clustered sources to the shape of the $P(D)$ does not affect only the sources brighter than the one-source-per-beam level, but all sources equally. Clusters of very faint sources might produce significant dispersion in the XRB intensity. As will be shown later, the effect of clustering is weighted by the X-ray volume emissivity as a function of redshift.

Fortunately, in most situations the $P(D)$ shape is dominated by the confusion noise of relatively bright sources, and the effect of clustering is only a small correction. In those cases it has been customary to parametrize the effect of clustering in terms of 'excess fluctuations', i.e., a small quantity ($\Delta I/I$) to be quadratically added to the intrinsic dispersion of the $P(D)$ (equation 1). In what follows we shall assume this approach.

The key point of this paper is based on the fact that the measurement of the variance of an approximately Gaussian distribution [we can use that approximation for $P(D)$ for this particular purpose] is distributed as χ^2. Therefore the 2σ uncertainty with which the dispersion of the $P(D)$ can be measured is $(2/N_{\rm obs})^{1/2}$ times the dispersion itself, where $N_{\rm obs}$ is the number of independent observations of the XRB intensity. That means that the 2σ sensitivity at which excess fluctuations could be measured is

$$\left(\frac{\Delta I}{I}\right)_{2\sigma} = \sqrt{\frac{2}{N_{\rm obs}}}\,\frac{(\sigma_{\rm c}^2+\sigma_{\rm ph}^2)^{1/2}}{I_{\rm XRB}}. \tag{2}$$

If we have a beam with solid angle Ω deg^2, and the whole high galactic latitude sky ($|b|>20°$) is used, then this number is $\sim 0.01\Omega^{1/2}(\Delta I/I)_{\rm intrinsic}$, which is why all-sky coverage is essential.

It should be emphasized that equation (2) shows the *maximum* precision that can be reached, and it requires knowledge of the intrinsic dispersion (equation 1) to better than this figure. In what follows we estimate these values on general grounds.

We assume a proportional counter with collimated field of view of solid angle Ω deg^2, effective area $10^4 A_4$ cm^2, with an energy bandpass from ϵ_1 to ϵ_2. For most purposes we will use $\epsilon_1=2$ keV and $\epsilon_2=10$ keV. This instrument is assumed to scan the whole sky in 6 months, so the typical exposure time will be of the order of $t=100\,t_{100}\Omega^{1/2}$ s.

2.1 Photon counting noise

Proportional counters detect events from the cosmic XRB as well as from particles crossing the detector. These have different energy spectra: the XRB has an energy spectrum $I_{\rm XRB}\propto\epsilon^{-0.4}$, which should be folded through the appropriate instrumental response (assumed as a constant effective area here) to be converted to counts, while the particle background is often well approximated by a constant energy dependence in the number of counts detected. If we write the total count rate as the sum of these two terms,

$$C_{\rm Tot}=C_{\rm XRB}+C_{\rm DET}, \tag{3}$$

then

$$C_{\rm XRB}=a_1\Omega A_4\Psi(-0.4,\,\epsilon_1,\,\epsilon_2) \tag{4}$$

and

$$C_{\rm DET}=a_2 A_4\Psi(1,\,\epsilon_1,\,\epsilon_2), \tag{5}$$

where we take into account bandpass corrections through the function Ψ:

$$\Psi(\beta,\,\epsilon_1,\,\epsilon_2)=\frac{\epsilon_2^{\beta}-\epsilon_1^{\beta}}{10^{\beta}-2^{\beta}}. \tag{6}$$

The constants a_1 and a_2 are more or less universal for the same type of orbit. We have estimated their values based on the *Ginga* LAC and the *RXTE* PCA. For the *Ginga* LAC ($A_4=0.4$, $\Omega=2$, $\epsilon_1=4$, $\epsilon_2=12$), $C_{\rm XRB}\sim 8$ count s^{-1} and $C_{\rm Tot}\sim 14$ count s^{-1} (see, e.g., Carrera et al. 1993), while for

RXTE ($A_4=0.14$, $\Omega=1$, $\epsilon_1=2$, $\epsilon_2=10$), $C_{\rm XRB}\sim 2.5$ count s^{-1} and $C_{\rm Tot}\sim 5$ count s^{-1} (K. Jahoda, private communication). From both instruments we find consistent values around $a_1\approx a_2\approx 15$–17 count s^{-1}.

The photon counting noise contribution to the dispersion of the $P(D)$ curve can then be estimated as

$$\left(\frac{\sigma_{\rm ph}}{I_{\rm XRB}}\right)=0.024\,(A_4 t_{100})^{-1/2} \times\left[\frac{1}{\Omega\Psi(-0.4,\,\epsilon_1,\,\epsilon_2)}+\frac{\Psi(1,\,\epsilon_1,\,\epsilon_2)}{\Omega^2\Psi^2(-0.4,\,\epsilon_1,\,\epsilon_2)}\right]^{1/2}. \quad (7)$$

The accuracy of this value depends crucially on how stable the particle background is around the orbit, and on whether it can be subtracted rather than modelled (this requires collimators of various sizes). An equatorial orbit minimizes variations due to the particle background.

2.2 Confusion noise

In what follows we assume that the source counts dominating the confusion noise follow a Euclidean power law

$$\frac{{\rm d}N}{{\rm d}S}=K\Omega(\gamma-1)\,\frac{1}{S_0}\left(\frac{S}{S_0}\right)^{-\gamma}, \quad (8)$$

where $\gamma=2.5$, S_0 is a reference flux arbitrarily chosen to be 10^{-14} erg cm^{-2} s^{-1} (2–10 keV), and the normalization $K=300\ K_{300}$ source deg^{-2} is the number of sources per square degree brighter than S_0. Both the slope and the normalization of the source counts are consistent with the fluctuation analysis carried out with the *Ginga* LAC (Butcher et al. 1997) and also match the deeper *ASCA* surveys (Inoue et al. 1996; Georgantopoulos et al. 1997), all of them referred to the 2–10 keV band. The spectrum of the *Ginga* LAC fluctuations also showed that the sources responsible for the confusion noise on 1-deg^2 scales have a power-law spectrum with energy spectral index 0.7 and negligible absorption (Butcher et al. 1997).

Confusion noise can be estimated following Condon (1974). If beams with an intensity more than $\Gamma\sigma$ above the mean are removed, since they will be identified as sources, the variance of the remaining map can be estimated iteratively and the confusion noise (defined as the flux equivalent to a 1σ signal in the intensity histogram) is

$$\sigma_{\rm c}=S_0\left(K\Omega\,\frac{\gamma-1}{3-\gamma}\,\Gamma^{3-\gamma}\right)^{1/(\gamma-1)}, \quad (9)$$

which, for a typical value $\Gamma\approx 5$ and Euclidean counts, is

$$\sigma_{\rm c}\sim 1.6\times 10^{-12}\ {\rm erg\ cm^{-2}\ s^{-1}}\ (K_{300}\Omega)^{2/3}. \quad (10)$$

This confusion noise produces a contribution to the intrinsic dispersion of the $P(D)$ curve,

$$\frac{\sigma_{\rm c}}{I_{\rm XRB}}=0.13\,K_{300}\Omega^{-1/3}\,\frac{\Psi(-0.7,\,\epsilon_1,\,\epsilon_2)}{\Psi(-0.4,\,\epsilon_1,\,\epsilon_2)}, \quad (11)$$

which will have to be added in quadrature to equation (7) to find the total intrinsic dispersion of the $P(D)$ curve.

A very important point is to what degree of accuracy this term can be estimated, since it is likely to be the main limiting factor to measurement of excess fluctuations. It is indeed important to have an all-sky survey (as *ABRIXAS* will provide) in order to minimize the statistical errors on this quantity. Over 8500 K_{300} sources are expected at high galactic latitudes down to a flux of 10^{-12} erg cm^{-2} s^{-1}, which would mean an accuracy of the order of 1 per cent in K and slightly better for $\sigma_{\rm c}$.

However, there is the issue of the source variability. AGN, which are supposed to be the dominant class of source at a flux 10^{-12} erg cm^{-2} s^{-1}, are known to vary substantially on all time-scales. Assuming that sources vary independently of each other and with a similar (flux-independent) amplitude, the measured source counts in a flux-limited sample are slightly different from the average source counts [which are relevant to the $P(D)$]. The main reason is that the steepness of the source counts makes a fraction of the sources of average flux below the detection threshold contribute to the source counts above the detection threshold. Indeed, some of the sources of average flux above the detection threshold would also be undetectable, but these are less numerous. The net result is that the source counts in a flux-limited sample are an overestimate of the average source counts, and it is this consideration which matters for the confusion noise.

In order to quantify the variability effect on the confusion noise, we have simulated fluxes of sources, whose average values are drawn from the source counts given by equation (8) down to 3×10^{-13} erg cm^{-2} s^{-1}. The number of simulated sources is set to cover the whole high galactic latitude sky in order to mimic the *ABRIXAS* survey. The fluxes are then allowed to vary randomly within a factor of a few. That produces a different list of source fluxes, which is then cut at 10^{-12} erg cm^{-2} s^{-1}. The source counts are then fitted via maximum likelihood to a single power law (as in equation 8), resulting in an estimate of the confusion noise given in equation (9).

Fig. 1 displays the relative variation between fitted and expected confusion noise as a function of input slope γ for $K_{300}=1$ when all sources vary within a factor of 2 and a factor of 5. The amount of overestimation of the confusion noise is ~ 1 per cent for Euclidean counts if sources vary within a factor of 2 and, as expected, it grows with γ. Since not all of the sources vary (there will be some contribution in the source counts from clusters of galaxies, galaxies, etc.) the error is likely to be smaller. For Euclidean counts the error is therefore small enough to reach the maximum accuracy in the excess fluctuations, assuming source variability within a factor of 2. The situation is clearly worse if sources vary within a factor of 5, where for Euclidean counts the variation in the confusion noise will be of the order of 5 per cent. There are indications (R. S. Warwick, private communication) that source variability could be large on average (close to a factor of 5) from the comparison of *ROSAT* All-Sky Survey data with later pointed observations. However, since variability produces a systematic effect on the confusion noise, different observations carried out by *ABRIXAS* (e.g., observations taken 6 months apart) of the same sources could be used to quantify this effect and to correct the source counts.

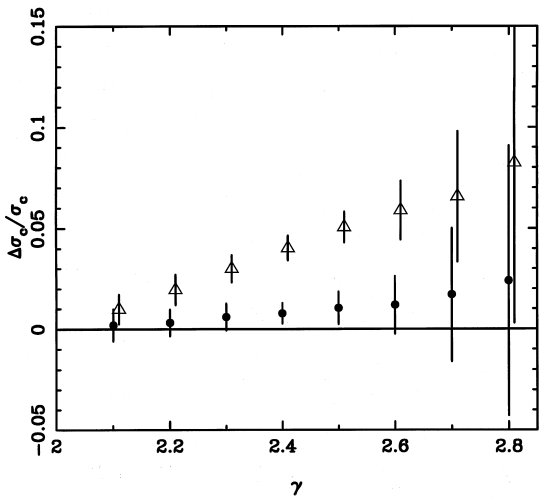

Figure 1. Relative shift in the estimates of confusion noise from an all-sky survey as a function of the slope of the differential source counts. Filled dots correspond to a factor of 2 variability, and triangles to a factor of 5 variability (these have been slightly shifted to higher values of γ to avoid confusion between error bars). The error bars represent the standard dispersion due to statistics and variability.

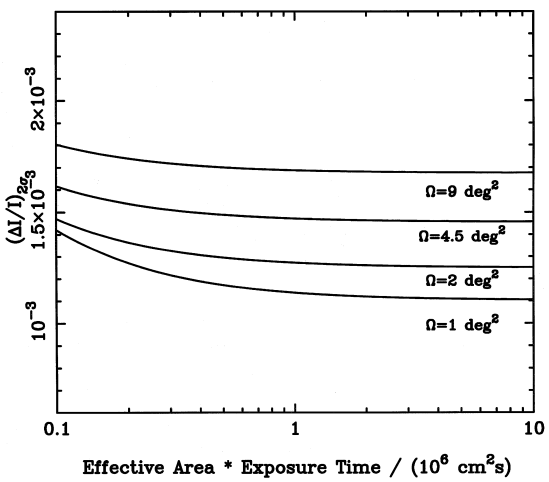

Figure 2. Minimum detectable excess variance for all-sky observations and different beamsizes.

2.3 Sensitivity to excess fluctuations

Equation (1), when combined with equation (11), shows that the minimum intrinsic dispersion in the $P(D)$ curve for a $\sim$1-deg set of observations is around 10 per cent. The accuracy with which any excess variance could be measured on top of this intrinsic value depends on the precision with which this dominating term can be modelled. If the intrinsic dispersion can be modelled to better than 1 per cent (which is close to the maximum statistical accuracy in the absence of source variability), then excess variances as low as $\sim 10^{-3}$ could be detected.

More precisely, and taking into account the estimated values for the confusion and photon counting noise from the previous subsections and assuming that source variability is not going to dominate the precision with which confusion noise can be estimated, the excess fluctuations that could be eventually measured by an all-sky observation with a collimated field-of-view proportional counter are shown in Fig. 2. This assumes a 2–10 keV bandpass.

Clearly, when the product $A_4 t_{100}$ is larger than a few (the precise value depending on the beam Ω), the intrinsic dispersion of $P(D)$ is dominated by confusion noise, as opposed to the photon counting noise which dominates at smaller values. When $P(D)$ is confusion-dominated, excess variances as small as 2×10^{-3} could be measured even with relatively large beams. For $\Omega=1$, values close to 1×10^{-3} would be within reach.

3 MEASURING THE POWER SPECTRUM OF THE FLUCTUATIONS AT HIGH REDSHIFT

The excess variance can be related to the PS of the density fluctuations in the following way (see Barcons & Fabian 1988 and Carrera et al. 1997 for details):

$$\left(\frac{\Delta I}{I}\right)^2 = \frac{1}{4\sqrt{2\pi}}\,\frac{c}{H_0 I_{\rm XRB}^2}\int {\rm d}z\, F(z;\, q_0) \times \int {\rm d}^2 q \hat{G}^2(q) \left(\frac{2}{\pi}\right)^{3/2} \mathscr{P}\,[z;\, q/d_{\rm A}(z)], \qquad (12)$$

where the XRB intensity $I_{\rm XRB}$ is

$$I_{\rm XRB} = \frac{\Omega_{\rm eff}}{4\pi}\,\frac{c}{H_0}\int {\rm d}z\,(1+z)^{-5}(1+2q_0 z)^{-1/2} j(z). \qquad (13)$$

$\Omega_{\rm eff}=3.046\times10^{-4}\Omega$, $j(z)$ is the X-ray volume emissivity at redshift z (with the appropriate K-correction), $d_{\rm A}$ is the angular distance,

$$d_{\rm A}(z) = \frac{c}{H_0}\,\frac{[zq_0+(q_0-1)(-1+\sqrt{1+2q_0 z})]}{q_0^2(1+z)^2}, \qquad (14)$$

$\hat{G}(q)$ is the 2D Fourier transform of the beam function, and $\mathscr{P}(z;\, k)$ is the PS of the fluctuations [$k\equiv(1+z)k_{\rm c}$ is the *physical* wavevector], which is related to the source two-point correlation function $\xi(z;\, r)$ by

$$\left(\frac{2}{\pi}\right)^{3/2}\mathscr{P}(z;\, k) = \frac{1}{(2\pi)^{3/2}}\int {\rm d}^3 r\, {\rm e}^{-{\rm i}k\cdot r}\,\xi(z;\, r), \qquad (15)$$

and, finally,

$$F(z;\, q_0) = (1+z)^{-8}(1+2q_0 z)^{-1/2} j^2(z)/d_{\rm A}^2(z). \qquad (16)$$

The above equations provide the basic link between excess fluctuations, evolution in the X-ray volume emissivity (the actual normalization is irrelevant since it cancels out) and the PS. Although the PS enters in the expression of the excess fluctuations in a convoluted way, there are a couple of simplifications that provide an almost one-to-one relation between the PS and excess fluctuations.

In what follows a circular beam with Gaussian profile (dispersion angle θ_0) will be assumed.

The first simplification to realize is that only wavevectors $k\sim\Omega_{\rm eff}^{-1/2} d_{\rm A}(z)^{-1}$ are relevant. The effective filtering

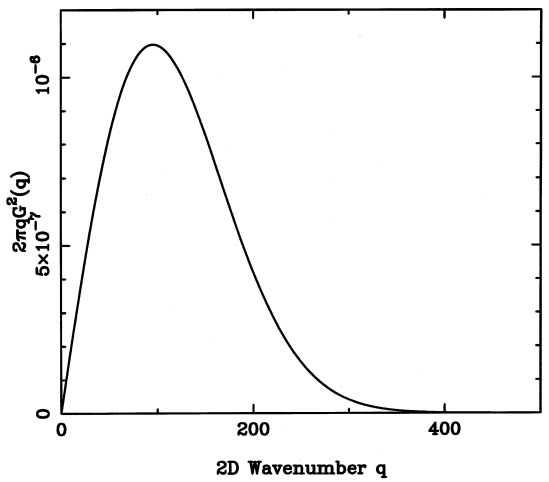

Figure 3. Effective beam filtering function for a 1° FWHM circular beam with Gaussian profile as a function of the 2D wavevector.

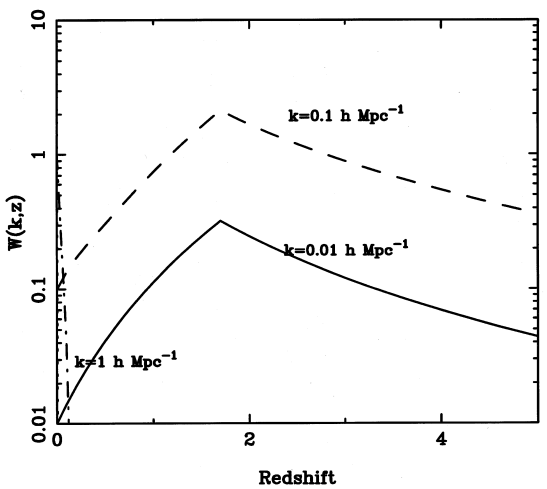

Figure 4. The weight $W(k, z)$ defined in equation (19) as a function of redshift for representative values of k.

function $2\pi q\hat{G}^2(q)$ is shown in Fig. 3 for a 1-deg FWHM beam (i.e., $\theta_0 = 1/2.354$ deg). It can be seen that only values of the 2D wavevector q around the maximum $q_{\max} = 2^{-1/2}\theta_0^{-1} \sim 100\Omega^{-1/2}$ deg^{-1} will contribute to the excess fluctuations. That implies that at every redshift z, only the 3D wavevectors $k \sim q_{\max}/d_A(z)$ will contribute substantially to the excess fluctuations. For beamsizes of the order of a degree, and significant redshifts $z \sim 1$, the 3D wavevectors to which it is maximally sensitive are $k \sim 0.01$–$0.1\ h$ Mpc^{-1}, which is near the expected maximum of the PS. Then, it is safe to assume that the PS does not vary much over the range of relevant wavevectors, which results in the following expression for the excess fluctuations:

$$\left(\frac{\Delta I}{I}\right)^2 = \int \mathrm{d}z \mathscr{W}(z) \mathscr{P}(z; [2^{1/2}\theta_0 d_A(z)]^{-1}), \tag{17}$$

where

$$\mathscr{W}(z) = \frac{2H_0}{c\Omega_{\mathrm{eff}}} \frac{(1+z)^{-8}(1+2q_0z)^{-1/2} j^2(z)/d_A^2(z)}{[\int \mathrm{d}z'(1+z')^{-2}(1+2q_0z')^{-1/2} j(z')]^2}. \tag{18}$$

The next simplification is hinted at by our (limited) knowledge of the redshift evolution of the X-ray volume emissivity $j(z)$. It is hoped that after *AXAF* and *XMM* are launched, and deep surveys have been carried out, optical identification work (especially for the *AXAF* sources whose positions will be determined with very good accuracy) will be able to reveal the volume emissivity $j(z)$ as a function of redshift. So far, at soft energies it appears that AGN have a steeply rising volume emissivity [$j(z) \propto K(z)(1+z)^{3+p}$, $K(z)$ being the K-correction and $p \sim 3$] up to $z_c = 1.7$, but beyond that redshift everything is consistent with no evolution (Boyle et al. 1994; Page et al. 1996). The NLXGs that appear to be more numerous at faint fluxes might also show a similar behaviour (Griffiths et al. 1996). To our present knowledge, then, $j(z)$ is a steeply rising function up to some redshift z_c and then it flattens out to a constant comoving volume emissivity.

In practice, that means that the influence of the PS (i.e., inhomogeneities in the distribution of sources) on the excess fluctuations is heavily weighted towards z_c for wavevectors $k < 0.1\ h$ Mpc^{-1}. In order to illustrate this fact, we define the function $W(k, z)$ by

$$\left(\frac{\Delta I}{I}\right)^2 = \int \mathrm{d}k \int \mathrm{d}z\, W(k, z)\, \mathscr{P}(z; k). \tag{19}$$

Fig. 4 shows $W(k, z)$ for different values of k assuming $p = 3$, an energy spectral index $\alpha = 1$ for the sources to compute the K-correction [the actual energy spectral index is likely to be smaller, and therefore the function $W(k, z)$ will be much more peaked towards z_c] and $z_c = 1.7$. What is seen there is that the wavevectors that dominate are around $k \sim 0.1\ h$ Mpc^{-1} and that within these, it is the redshift at which the volume emissivity peaks that is most heavily weighted. There is, of course, some contribution from smaller wavevectors at lower redshifts, but since the peak in the PS is expected to be found around these shorter wavevectors, not much contamination from large-scale local structure is to be expected. In fact, this large-scale power could be removed by 'flat-fielding' the all-sky maps with a large-scale smoothed version of the same maps, leaving scales of $k \sim 0.1\ h$ Mpc^{-1} unaffected. This would have the additional advantage of removing any residual Galactic large-scale structure. It is then concluded that we could be measuring the PS at a redshift beyond the deepest available galaxy surveys.

To estimate the sensitivity in the measurement of the PS with X-ray observations, we assume that all of the XRB comes from a redshift bin $\Delta z = 2$ around $z_c = 1.7$ and approximate the integrals in redshift as the central value of the integrand times Δz. We then find

$$\left(\frac{\Delta I}{I}\right)^2 = \frac{2}{\Delta V} \mathscr{P}(z_c; k_0), \tag{20}$$

where $k_0 = 2^{-1/2}\theta_0^{-1} d_A(z_c)^{-1}$, and ΔV is the volume sampled by a beam

$$\Delta V = \Omega_{\mathrm{eff}} d_A(z_c)^2 c H_0^{-1} (1+z)^{-2}(1+2q_0z)^{-1/2}\Delta z. \tag{21}$$

Fig. 5 shows the maximum sensitivity, in terms of the PS as a function of comoving wavevector, for different

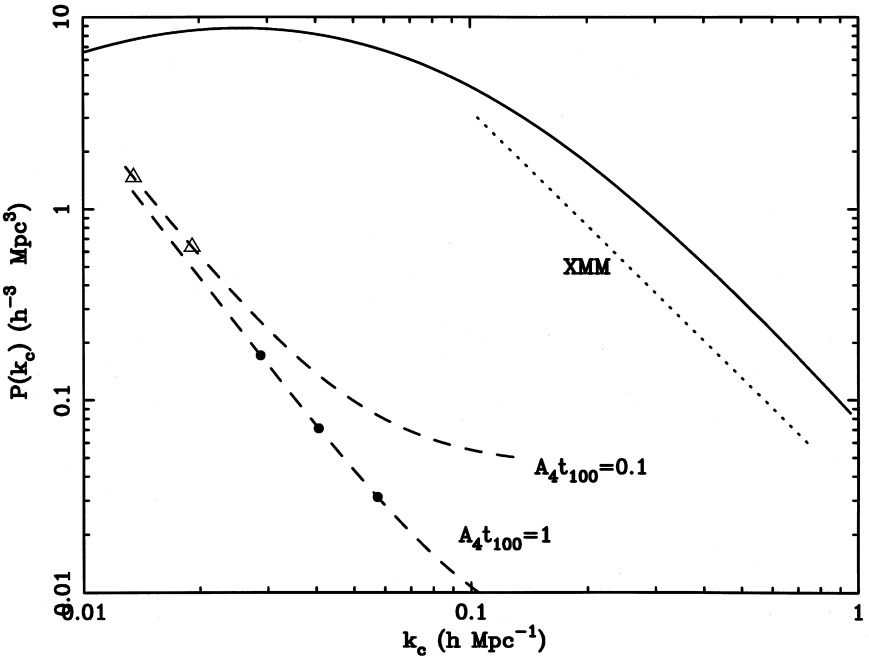

Figure 5. Power spectrum of density fluctuations as a function of comoving wavevector all computed at a redshift $z=1.7$. The solid line represents the prediction from local observations evolved with $q_0=0.5$. The dashed curves are the 2σ sensitivities from all-sky surveys carried out with various beamsizes and for the quoted values of the parameter A_4t_{100}. The triangles show the maximum sensitivity that could be reached with *HEAO-1 A2* data (for the $3°\times3°$ and $1.°5\times3°$ collimators from left to right), and the filled circles show the sensitivity of the instrument whose concept is presented in Section 4.1, with beamsizes of 2, 1 and 0.5 deg^2 (left to right). The dotted line shows the sensitivity of XMM observations for 2 yr, as explained in the text.

beamsizes, according to the estimates from Section 2. A factor of 2 reduction in the number of independent measurements has been included in order to account for the fact that neighbouring observations will not be independent. For the *HEAO-1 A2* points (triangles) $A_4t_{100}=0.1$. The dashed lines represent the expected maximum sensitivities for all-sky observations of the XRB with different beamsizes (ranging from 10 to 0.1 deg^2 and various values of A_4t_{100}. The filled dots represent beams of 2, 1 and 0.5 deg^2 for $A_4t_{100}=1$, as in the instrument whose concept is presented in the next section. From this figure it is clearly seen that the best sensitivity near the expected peak of the PS is achieved by 0.5–1 deg^2 beams, and that to avoid the results being dominated by photon counting noise (i.e., the flattening of the dashed curves towards high wavevectors) at those angles, a value of A_4t_{100} close to 1 is needed.

In the same figure we also show the expected sensitivity reached at larger wavevectors with *XMM* observations over 2 yr. That has been computed assuming a $\log N$–$\log S$ as observed at soft X-ray energies with $\gamma=2$, but with a normalization two times larger, as it seems to apply to the 2–10 keV passband (Georgantopoulos et al. 1997). We have assumed about 500 useful observations with an average exposure time of 20 ks during that period.

We also show for comparison a CDM PS (see Peacock 1997 and in particular fig. 6 of that paper) linearly evolved to redshift 1.7 (with $q_0=0.5$). A shape parameter $\Gamma^*=0.25$ has been assumed, claimed by Peacock & Dodds (1994) to fit the shape of the local LSS very well, and the normalization has been chosen accordingly. The conclusion is that when the confusion noise from sources brighter than $\sim10^{-12}$ erg cm^{-2} s^{-1} can be accurately modelled, the all-sky *HEAO-1 A2* observations might be sensitive enough to measure the PS at intermediate redshift (that is in the absence of other systematics). With a smaller beam (close to 0.5–1 deg^2) and larger area the accuracy in the measurement could be of a few per cent.

4 MEASURING THE XRB FLUCTUATIONS ON 1-DEGREE SCALE

4.1 A mission dedicated to the XRB

Throughout this paper we have illustrated what results would be obtained by using a beamsize close to 1 deg^2. In what follows we want to show how the simplest possible instrument (i.e., a collimated field-of-view proportional counter) could provide a very significant cosmological result.

Indeed, other instruments might provide, in principle, similarly valuable information with comparable sensitivity in terms of excess variance. For values of the product $A_4t_{100}>0.1$, the measurement of the fluctuations could be sensitive enough to provide cosmologically relevant results. We believe that systematics are going to dominate the ultimate sensitivity of such measurements. If unpredictable and slow gain variations in the instrument are the dominant source of the systematics, then the larger the effective area the better, especially when the measurement can be repeated a few times. A detailed study would be required for each experiment where systematics need to be understood and kept to a minimum. We devote here special atten-

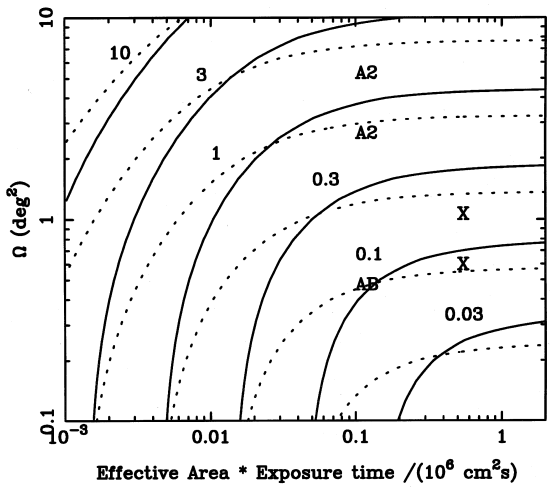

Figure 6. Contour levels of constant power spectrum (in h^{-3} Mpc^3 units) achievable at redshift $z_c = 1.7$. The solid lines represent the 2–10 keV bandpass, and the dotted lines the 1–5 keV bandpass. The two *HEAO-1 A2* collimator sizes (4.5 and 9 deg^2) have been labelled 'A2', while the instrument proposed here has been labelled 'X' (collimator sizes 1 and 23 deg^2). The *ABRIXAS* point, assuming an area of 25 cm^2 and a total integration time of 4000 s, is shown as 'AB'.

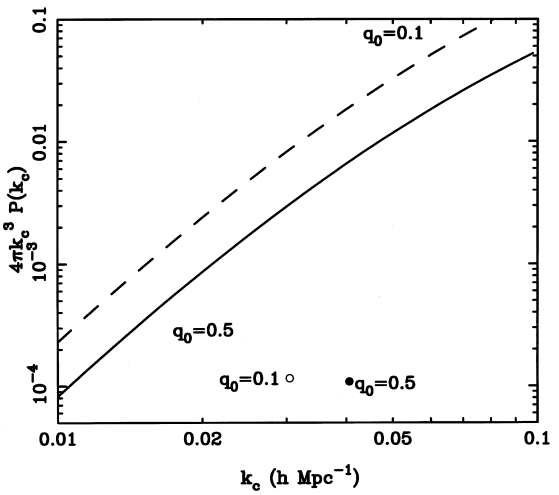

Figure 7. Dimensionless power spectrum (PS) estimated at different values of q_0. The solid curve corresponds to a linearly evolved $q_0 = 0.5$ local PS (see text). The dashed line shows the same thing for $q_0 = 0.1$. The filled and empty circles show the expected 2σ sensitivities from the observations suggested in Section 4.1 and for $q_0 = 0.5$ and 0.1 respectively.

tion to proportional counters which are well understood and have proven stable over extended periods.

Although the smallest detectable excess fluctuations $(\Delta I/I)_{2\sigma}$ for a 1-deg^2 experiment would be within a factor of 2 of what can be done with *HEAO-1 A2* (see Fig. 2), the sensitivity in the measurement of the PS would be increased by a much larger factor, since a much smaller volume ΔV would be sampled by a single beam (see equation 20). To illustrate this point further, we show in Fig. 6 what such an instrument would be able to do in terms of measuring the PS, as a function of the parameter $A_4 t_{100}$ and beam Ω. Fig. 6 also shows the expected values for a 1–5 keV bandpass which would collect more counts, but due to the fact that the sources that dominate the confusion noise have a steeper spectrum than the XRB, the $P(D)$ curves would be noisier and the experiment less sensitive.

We propose an instrument of effective area $A_4 = 1$, with two collimator sizes (1 and 2 deg^2) so that the contribution from cosmic and detector backgrounds could be well separated. It might be actually very interesting that the collimators are elongated (e.g., $0.^\circ5 \times 2^\circ$ and $1^\circ \times 2^\circ$), in which case there will be some information on the PS down to smaller scales. With such a large effective area, the X-ray brightness of the sky at any point could be determined with an accuracy better than 2 per cent. The PS at $k_c \sim 0.01$–$0.1\ h$ Mpc^{-1} could then be measured, in principle, down to $0.1\ h^{-3}$ Mpc^3 or better (2σ), which would guarantee not only a detection (if the PS at intermediate redshift is not largely overestimated by the above parametrization) but also an accurate measurement. In what follows we try to highlight the need for such an instrument, and also list a few complementary studies that would benefit considerably from such observations.

First of all, Figs 5 and 6 show the minimum detectable power spectra, assuming that the intrinsic width of the $P(D)$ can be determined to its absolute statistical precision. Indeed, it might be that source variability is found to have a larger effect or that photon counting noise cannot be modelled to 1 per cent accuracy. If one or both of these effects cause a 5 per cent uncertainty in the intrinsic $P(D)$ noise, then with the *HEAO-1 A2* experiment (degrading its sensitivity in the PS by almost an order of magnitude) the cosmic signal in the PS would be missed. A 5 per cent accuracy in the intrinsic $P(D)$ width with the proposed experiment would nevertheless allow a PS as small as ~ 2 h^{-3} Mpc^3 (still below the prediction) to be detected at 2σ. Indeed, the fact that such an instrument would be working close to the peak of the PS helps.

To illustrate the capabilities of this observation further, we explored the possibility that a sensitive measurement of the PS at intermediate redshift could constrain the evolutionary parameters of the PS. We have taken the $z = 0$ CDM spectrum with constant Γ^* (see Section 3 and Peacock 1997) and evolved it linearly (which is appropriate to the scales under consideration) to $z = 1.7$ with different values of q_0. The dimensionless PS [$4\pi k_c^3 \mathscr{P}(k_c)$; Fig. 7] does not depend on the Hubble constant h, but does depend on q_0. The expected 2σ accuracy for the dimensionless PS is between one and two orders of magnitude smaller than the predictions. The difference between the expected dimensionless power spectrum for $q_0 = 0.1$ and 0.5 is only a factor of 4 at that redshift, and therefore q_0 could be measured in principle.

Such a mission makes no severe technical demands requiring only a continuous scan of the whole sky over 2 yr with the most stable proportional counters and one-axis stabilization. In order to keep the contribution to the intrinsic dispersion of the $P(D)$ curve well determined, it is necessary to have the detector background as stable as possible. In this respect, the mission concept we propose here would be better suited if it were launched into an equatorial orbit (as for *BeppoSAX*).

4.2 Other ways to measure large-scale structure

There are many other scientific goals that could be achieved while such an instrument is performing its main task. Within the subject of the LSS, the multipoles of the XRB should be mentioned first. In fact, at least the dipole needs to be well measured and compared with the dipole in the distribution of the X-ray sources to estimate the bias parameter. The earliest attempts to measure LSS with the use of the XRB looked also for 12- and 24-h effects which could be attributed to the presence of a large lump of X-ray-emitting matter at different distances (Warwick et al. 1980). *HEAO-1 A2* provided the possibility of a measurement of the dipole of the XRB, whose direction is in general agreement (within large errors) with the CMB dipole (Shafer 1983; Shafer & Fabian 1983). The amplitude of the XRB dipole is expected to be larger than the CMB one, primarily because of aberration [$(\Delta I/I)_{\rm Dip}=(3+\alpha)\,v/c$, α being the energy spectral index; $\alpha\sim 0.4$ for the XRB, and $\alpha=-2$ for the CMB], but also because the mass overdensity which is gravitationally pulling the Local Group is also expected to emit X-rays above the average (Warwick et al. 1980; Miyaji & Boldt 1990; Boldt 1992; Miyaji 1995).

More recently, Lahav et al. (1997) have proposed a formalism to measure multipoles in the XRB and to relate them to the PS of the fluctuations, as is done with galaxy surveys. Of course, the main problem in measuring multipoles is not a sensitivity one, but confusion noise. The amplitude of the dipole is <1 per cent and must be measured in maps where confusion noise is larger. Since all the multipoles are, in fact, variances of the sky maps weighted with appropriate spherical harmonics, the contribution of confusion noise is dominated by the brightest sources that have not been removed. That makes the measurement of multipoles particularly difficult (Lahav, private communication). In addition, there is the unknown contribution of the Galaxy, even at high galactic latitudes which could contribute to the low-order (large-scale) multipoles.

There is, however, an advantage in the experiment proposed here with respect to the only previous one that carried out an all-sky survey (*HEAO-1 A2*), when combined with *ABRIXAS*. The 'shot noise' variance for all multipoles is (see Lahav et al. 1997)

$$\langle |a_{lm}|^2\rangle_{\rm sn}=S_0^2 K\Omega\,\frac{\gamma-1}{3-\gamma}\left(\frac{S_{\rm max}}{S_0}\right)^{3-\gamma}, \qquad (22)$$

where $S_{\rm max}$ is the flux above which all sources have been removed. If *ABRIXAS* can find the positions of all sources brighter than 10^{-12} erg cm^{-2} s^{-1}, whose surface density is 0.3 deg^{-2}, then one out of every three beams will have to be excluded from the multipole analysis. This still provides enough data, with virtually no impact on the amplitude of the multipole signal, but with the 'shot noise' reduced by a factor of 5, when compared with the *HEAO-1 A2* maps where the Piccinotti et al. (1982) sources have been removed.

The proposed mission will also provide a good measurement of the autocorrelation function. Since the instrument would scan the sky along great circles, measurements of the sky brightness at separations less than the collimator field of view will be taken. These can be used to measure the autocorrelation function of the XRB on scales smaller than the beamsize. However, since the beams will strongly overlap in adjacent measurements, the signal in the autocorrelation function will be dominated by the brightest sources present (see Martín-Mirones et al. 1991 and Carrera et al. 1993). At the very least, this will be useful to confirm the source counts at high fluxes (as was done, for example, in the *Ginga* High Galactic Latitude Survey by Kondo 1991). Beyond the angular scale where the beams overlap, the autocorrelation function is expected to measure true source clustering and extension of the cosmic sources. If clusters of galaxies can be reliably removed from the all-sky maps (again using *ABRIXAS*), source clustering on scales larger than the beamsize could also be measured.

Other possibilities for such an instrument include the search for positive or negative signals around known structures (the Great Attractor, superclusters, voids, etc.), studies of the cross-correlation function between XRB intensity and galaxy and cluster catalogues (Jahoda et al. 1991; Lahav et al. 1993a; Miyaji et al. 1994; Barcons et al. 1995; Carrera et al. 1995; Sołtan et al. 1996) as well as with X-ray maps at softer energies, cross-correlations of the XRB with CMB maps (Boughn & Jahoda 1993; Boughn et al. 1997; Kneissl et al. 1997), possible detection of excess skewness in the fluctuations (similar to what is done in counts-in-cells; Lahav et al. 1993b), and many types of studies of the distribution of X-ray sources and diffuse emission from the Galaxy.

5 CONCLUSIONS

We have shown that all-sky degree-scale observations of the XRB carried out with enough sensitivity (effective area times exposure time in excess of 10^6 cm^2 s) could reveal excess fluctuations due to the clustering of distant sources down to levels $(\Delta I/I)_{2\sigma}\sim(1\text{–}2)\times 10^{-3}$. These excess fluctuations are likely to arise from high-redshift sources, and then the power spectrum (PS) of the fluctuations at those early epochs could be measured with sufficient sensitivity to detect the cosmic signal.

The generic requirement for such a goal is that the intrinsic width of the $P(D)$ curve (caused by confusion noise and photon counting noise) is estimated to better than 1 per cent. Source variability (if within a factor of 2) already introduces a bias of 1 per cent for Euclidean source counts if an all-sky survey of sources brighter than 10^{-12} erg cm^{-2} s^{-1} is used (as will be carried out by *ABRIXAS*). If variability is as large as a factor of 5, then the contribution of confusion noise to the intrinsic $P(D)$ dispersion will suffer from a 5 per cent error. Besides this, photon counting noise needs to be modelled to better than 1 per cent to achieve the maximum sensitivity in the excess fluctuations.

When the X-ray source counts down to that flux have been measured, the $P(D)$ noise in the *HEAO-1 A2* maps could be accurately modelled, and the PS of the density fluctuations at intermediate redshift might be measurable if the modelling of $P(D)$ can be done accurately enough.

A new X-ray mission consisting of a large effective area proportional counter with 1- and 2-deg^2 collimators, which would scan the whole sky several times, would provide a much more secure approach. Such an experiment would have a sensitivity 10 times better in terms of the PS than the

HEAO-1 A2 experiment and would be able to detect a signal in the PS over 10–100 times smaller than the predictions of the popular models. We believe that such an experiment constitutes the best chance to measure the PS of the density fluctuations in the Universe at a redshift $z \sim 1$–2, where the different cosmological scenarios give the most distinct predictions.

ACKNOWLEDGMENTS

We thank Elihu Boldt, Günther Hasinger, Keith Jahoda, Ofer Lahav and Bob Warwick for their comments about the concept presented in Section 4.1, which resulted in substantial improvements which propagated throughout the paper. Partial financial support for XB and FJC was provided by the DGES under project PB95-0122. Financial help for XB's sabbatical at Cambridge was provided by DGES grant PR95-490. ACF thanks the Royal Society for support.

REFERENCES

Barcons X., 1992, ApJ, 396, 460
Barcons X., Fabian A. C., 1988, MNRAS, 230, 189
Barcons X., Fabian A. C., 1990, MNRAS, 243, 366
Barcons X., Branduardi-Raymont G., Warwick R. S., Fabian A. C., Mason K. O., McHardy I. M., Rowan-Robinson M., 1994, MNRAS, 268, 833
Barcons X., Franceschini A., De Zotti G., Danese L., Miyaji T., 1995, ApJ, 455, 480
Boldt E., 1987, Phys. Rep., 145, 215
Boldt E., 1992, in Barcons X., Fabian A. C., eds, The X-ray Background. Cambridge Univ. Press, Cambridge, p. 115
Boughn S. P., Jahoda K., 1993, ApJ, 412, L1
Boughn S. P., Crittenden R. G., Turok N. G., 1997, New Astron., submitted
Boyle B. J., Mo H. J., 1993, MNRAS, 260, 925
Boyle B. J., Shanks T., Georgantopoulos I., Stewart G. C., Griffiths R. E., 1994, MNRAS, 271, 639
Butcher J. A. et al., 1997, MNRAS, 291, 437
Carrera F. J., Barcons X., Butcher J. A., Fabian A. C., Stewart G. C., Warwick R. S., Hayashida K., Kii T., 1991, MNRAS, 249, 698
Carrera F. J. et al., 1993, MNRAS, 260, 376
Carrera F. J., Barcons X., Butcher J. A., Fabian A. C., Lahav O., Stewart G. C., Warwick R. S., 1995, MNRAS, 275, 22
Carrera F. J., Fabian A. C., Barcons X., 1997, MNRAS, 285, 820
Condon J. J., 1974, ApJ, 188, 279
Cress C. M., Helfand D. J., Becker R. H., Gregg M. D., White R. L., 1996, ApJ, 473, 7
Cristiani S., D'Odorico S., D'Odorico V., Fontana A., Giallonago E., Savaglio S., 1997, MNRAS, 285, 209
Croom S. M., Shanks T., 1996, MNRAS, 281, 893
Fernández-Soto A., Lanzetta K. M., Barcons X., Carswell R. F., Webb J. K., Yahil A., 1996, ApJ, 460, L85
Friedrich P. et al., 1996, in Zimmermann H. U., Trümper J., Yorke H., eds, Röntgenstrahlung from the Universe. MPE Report 263, p. 681
Le Fèvre O., Hudon D., Lilly S. J., Crampton D., Hammer F., Tresse L., 1996, ApJ, 461, 534
Georgantopoulos I., Stewart G. C., Blair A. J., Shanks T., Griffiths R. E., Boyle B. J., Almaini O., Roche N., 1997, MNRAS, 291, 203
Giacconi R., Gursky H., Rossi B., Paolini F., 1962, Phys. Rev. Lett., 9, 439
Griffiths R. E., Della Ceca R., Georgantopoulos I., Boyle B. J., Stewart G. C., Shanks T., Fruscione A., 1996, MNRAS, 281, 71
Hamilton T. T., Helfand D. J., 1987, ApJ, 318, 93
Hasinger G., 1996, A&AS, 120, 607
Hasinger G., Burg R., Giacconi R., Hartner G., Schmidt M., Trümper J., Zamorani G., 1993, A&A, 275, 1
Hayashida K., 1989, PhD thesis, Univ. Kyoto
Inoue H., Kii T., Ogasaka Y., Takahashi T., Ueda Y., 1996, in Zimmermann J. U., Trümper J., Yorke H., eds, Röntgenstrahlung from the Universe. MPE Report 263, p. 323
Iwan D., Shafer R. A., Marshall F. E., Boldt E. A., Mushotzky R. F., Stottlemeyer A., 1982, ApJ, 260, 111
Jahoda K., Mushotzky R. F., 1989, ApJ, 346, 638
Jahoda K., Mushotzky R. F., Boldt E. A., Lahav O., 1991, ApJ, 378, L37; Erratum: 1992, ApJ, 399, L107
Kneissl R., Egger R., Hasinger G., Sołtan A. M., Trümper J., 1997, A&A, 320, 685
Kondo H., 1991, PhD thesis, Univ. Tokyo
Lahav O. et al., 1993a, Nat, 364, 693
Lahav O., Itoh M., Inagaki S., Suto Y., 1993b, ApJ, 402, 387
Lahav O., Piran R., Treyer M. A., 1997, MNRAS, 284, 499
Loan A., Wall J. V., Lahav O., 1997, MNRAS, 286, 994
Martín-Mirones J. M., De Zotti G., Franceschini A., Boldt E. A., Marshall F. E., Danese L., Persic M., 1991, ApJ, 379, 507
Miyaji T., 1995, PhD thesis, Univ. Maryland
Miyaji T., Boldt E., 1990, ApJ, 353, L3
Miyaji T., Lahav O., Jahoda K., Boldt E., 1994, ApJ, 434, 424
Mushotzky R. F., Jahoda K., 1992, in Barcons X., Fabian A. C., eds, The X-ray Background. Cambridge Univ. Press, Cambridge, p. 80
Page M. J. et al., 1996, MNRAS, 281, 579
Peacock J. A., 1997, MNRAS, 284, 885
Peacock J. A., Dodds S. J., 1994, MNRAS, 267, 1020
Persic M., Jahoda K., Rephaeli Y., Boldt E., Marshall F. E., Mushotzky R. F., Rawley G., 1990, ApJ, 364, 1
Piccinotti G., Mushotzky R. F., Boldt E. A., Holt S. S., Marshall F. E., Serlemitsos P. J., Shafer R. A., 1982, ApJ, 253, 485
Scheuer P. A. G., 1957, Proc. Cambridge Phil. Soc., 53, 764
Scheuer P. A. G., 1974, MNRAS, 166, 329
Shafer R. A., 1983, PhD thesis, Univ. Maryland
Shafer R. A., Fabian A. C., 1993, in Abell G. O., Chincarini G., eds, Proc. IAU Symp. 104, Early Evolution of the Universe and its Present Structure. Reidel, Dordrecht, p. 333
Sołtan A. M., Hasinger G., Egger R., Snowden S., Trümper J., 1996, A&A, 305, 17
Voges W., 1993, Adv. Space Res., 131, 391
Warwick R. S., Pye J., Fabian A. C., 1980, MNRAS, 190, 243